

A Comparative Analysis of Wealth Index Predictions in Africa between three Multi-Source Inference Models^{*}

Márton Karsai^{1,3}[0000–0001–5382–8950], János Kertész^{1,2}[0000–0003–4957–5406],
and Lisette Espín-Noboa^{2,1} (✉)[0000–0002–3945–2966]

¹ Central European University, Vienna 1100, Austria
{KarsaiM,KerteszJ,EspinL}@ceu.edu

² Complexity Science Hub, Vienna 1080, Austria

³ National Laboratory for Health Security, HUN-REN Alfréd Rényi Institute of Mathematics, Budapest 1053, Hungary

Abstract. Poverty map inference is a critical area of research, with growing interest in both traditional and modern techniques, ranging from regression models to convolutional neural networks applied to tabular data, images, and networks. Despite extensive focus on the validation of training phases, the scrutiny of final predictions remains limited. Here, we compare the Relative Wealth Index (RWI) inferred by Chi et al. (2022) with the International Wealth Index (IWI) inferred by Lee and Braithwaite (2022) and Espín-Noboa et al. (2023) across six Sub-Saharan African countries. Our analysis focuses on identifying trends and discrepancies in wealth predictions over time. Our results show that the predictions by Chi et al. and Espín-Noboa et al. align with general GDP trends, with differences expected due to the distinct time-frames of the training sets. However, predictions by Lee and Braithwaite diverge significantly, indicating potential issues with the validity of the models. These discrepancies highlight the need for policymakers and stakeholders in Africa to rigorously audit models that predict wealth, especially those used for decision-making on the ground. These and other techniques require continuous verification and refinement to enhance their reliability and ensure that poverty alleviation strategies are well-founded.

1 Introduction

Accurate and detailed poverty maps are indispensable for targeting anti-poverty interventions. While the United Nations prioritizes poverty eradication [26], official poverty maps often do not exist [22] or lack the granularity to identify specific areas of critical need due to data aggregation at broad administrative levels [25]. In recent years, predicting poverty using novel data sources has garnered significant attention within the AI for social good community. Diverse approaches leveraging satellite imagery [10,14], mobile phone data [4,6], social media activity [18,20], or combinations thereof [2,17,8], have emerged, raising questions

^{*} Please cite the ECMLPKDD’24 version of this paper

about the optimal methodology for accurate poverty estimation. Towards this goal, Espín-Noboa et al. 2023 [8] examined the performance of three machine learning architectures utilizing satellite imagery, tabular data, and a hybrid approach. Their findings revealed a nuanced landscape, with image-based models excelling at inferring the wealthiest areas, while tabular features proved more effective in rural regions. These findings highlight the importance of tailoring models to specific regions and feature sources.

However, current methods for creating poverty maps have some limitations. Although model architectures, features, and train-test validations are meticulously designed and evaluated on small samples, they may not ensure accurate predictions in the final poverty maps. The lack of ground-truth data prevents the validation of these predictions, leading to potential inaccuracies. Consequently, these unvalidated predictions are used for policy-making, relying on training samples that may not accurately represent the entire population.

Another critical issue is the choice of ground-truth indicators. Various studies use socioeconomic indicators such as income per capita [7], housing prices [27], and wealth indexes [2,17,8], each with its strengths and limitations [21]. Different wealth indexes such as the Relative Wealth Index (RWI), the Comparative Wealth Index (CWI), the Harmonized Wealth Index (HWI), and the International Wealth Index (IWI), provide distinct perspectives on wealth but also come with inherent constraints [17]. This variability makes it challenging to determine the most reliable inferred poverty map when comparing methodologies with similar predictive power.

If the validations of these different models are equally accurate, their resulting poverty maps should theoretically be similar. However, any discrepancies would prompt an investigation into the reasons for these differences and an assessment of which model is more accurate. In this study, we aim to address this gap by comparing three recent wealth inference approaches: **RWI** by Chi et al. [2], and **IWI** by Lee and Braithwaite [17], and by Espín-Noboa et al. [8]. We show their inferred poverty maps across six African countries and examine the degree of concordance of these predictions with established GDP trends, aiming to evaluate the robustness and reliability of these methodologies. The analysis is two-fold. First, we compare the predicted distributions of wealth to assess the overall poverty inferred for each country by each model. Second, considering the differences in geo-located places each approach uses in the final poverty map, we verify whether overlapping locations across methods receive consistent predictions and align with expected poverty trends. In adherence to open science practices, we make both the code and the predictions openly available [9].

2 Preliminaries

In this study, we compare the predictions of high-resolution poverty maps across six African countries from three different studies: **M1** by Chi et al. (2022) [2], **M2** by Lee and Braithwaite (2022) [17], and **M3** by Espín-Noboa et al. (2023) [8].

2.1 Ground-Truth Data

Ground-truth data in M1, M2, and M3 are derived from nationally-representative, population-based household surveys conducted by the Demographic and Health Survey (DHS) Program [13]. These surveys encompass asset/wealth information and sub-regional geomarkers. Each household survey includes numerous questions on socioeconomic status. From the responses, DHS calculates the Relative Wealth Index (RWI) [3,24] using the first principal component derived from a Principal Component Analysis (PCA) [12,15] of a standardized set of 15 questions concerning assets and housing characteristics. These questions cover various aspects such as electricity, telephone, automobile, refrigerator, TV, water supply, toilet facilities, and construction materials. This RWI serves as the ground-truth measure of wealth in M1. In contrast, M2 and M3 compute the International Wealth Index (IWI) [23], a similar metric, which assesses household material well-being and economic status across low and middle-income countries. The IWI is derived from 12 housing characteristics; M2 excludes two of them, while M3 uses them all. PCA is used to determine asset weights, which are re-scaled to produce IWI scores ranging from 0 to 100, representing the spectrum from no assets to the highest wealth. The IWI’s advantage lies in its comparability across different countries and years, unlike the country-specific RWI used in M1.

The studies also differ in their spatial resolution. M1 employs a 2.4 km grid system defined by Bing tile coordinates to map DHS clusters to grid cells. Conversely, M2 and M3 use actual DHS cluster locations which typically contain 25-30 households, and are geo-located with added noise to protect respondents privacy. The noise varies: up to 2 km for urban and 5 km for rural clusters, with 1% of rural clusters displaced by up to 10 km [1].

The final poverty map is defined by the grid-cells covering the entire country in M1, and by the populated places (i.e., cities, towns, villages, hamlets and isolated dwellings) extracted from OpenStreetMap (OSM) in M2 and M3 (M3 additionally includes neighborhoods).

Another critical difference among the three studies is the year in which the surveys were conducted. Each study utilized training data from different years (see Table 1), complicating the direct comparison of their results. Consequently, as explained in Section 2.3, our comparison will not concentrate on the precise predictions of each study. Instead, we will focus on identifying expected trends, using the Gini coefficient of wealth distributions and GDP per capita as baselines. These baselines are sourced from official data provided by the World Bank [28,29]. This approach allows us to account for temporal variations and provides a more meaningful analysis of the wealth and economic status trends across different periods.

2.2 Models

M1: RWI inference model by Chi et al. 2022 [2,5] utilizes 112 features in total, including high-resolution satellite imagery, mobile phone network data, topographic maps, and aggregated, de-identified connectivity data from Facebook.

Table 1: **Years of collected DHS ground-truth and features per study.** Instances where two or more models used the same ground-truth data are few: M2 and M3 in Uganda, M1 and M2 in Rwanda, and all models in South Africa. M2 inferred Gabon’s poverty map using a model trained on data from 25 Sub-Saharan African countries, as the most recent survey from 2012 was considered outdated. The table also categorizes the features utilized by each model. Note that for this analysis, unlike the original models reported in [8], the M3 models were retrained from scratch without mobility and demographic features, as the mobility data was discontinued and the Facebook Marketing API redefined its reach estimates. This change did not affect performance.

Country (ISO 3166-1 alpha-3 Code)	M1	M2	M3
Sierra Leone (SLE)	2013	2016	2016,2019
Liberia (LBR)	2013	2016	2019,2022
Uganda (UGA)	2016	2016,2018-19	2016,2018-19
Rwanda (RWA)	2014-15	2014-15	2019
South Africa (ZAF)	2016	2016	2016
Gabon (GAB)	2012	Multiple	2019
Feature	M1	M2	M3*
Daylight satellite images	✓	✓	✓
Nightlight intensity	✓	✓	✓
Infrastructure	✓	✓	✓
Connectivity	✓	-	✓
Population	✓	✓	✓
Mobility network †	-	-	(✓)
Demographics of people †	-	-	(✓)
Natural conditions	✓	-	-
Number of total features ‡	12+100	249+4	173+784

* This model has three variants: CNN (only images), CatBoost (all but images), and combined (all features).

† We exclude these features due to discontinued support (mobility) and rapid changes of API (demographics).

‡ Metadata (non-imagery) features (12, 249, and 173, resp.) plus image-based features (100, 4, and 784, resp.).

These diverse data sources are processed through deep learning and computational algorithms to generate quantitative features for each village. These features are then used to train a gradient-boosted regression tree, a supervised machine-learning model, to predict RWI scores. Hyperparameters for the gradient-boosted tree are tuned to minimize the cross-validated mean-squared error (MSE), using a grid search. They use three cross-validation approaches: 5-fold cross-validation (basic CV), leave-one-country-out cross-validation (leave-country-out), and spatially stratified cross-validation (spatial CV). The use of different cross-validation methods helped highlight the potential upward bias in performance due to spatial auto-correlation in the training and test data. All analysis in this study is based on spatial CV, ensuring conservative and appropriate model training for geographic data with spatial auto-correlation. For our

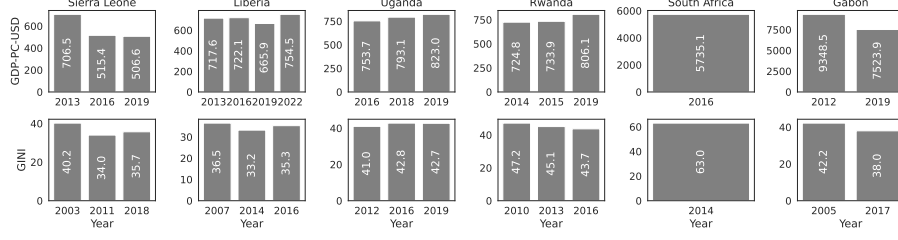


Fig. 1: **Available GDP per capita and Gini index.** Top: GDP values are aligned with the years of the surveys used in the models (x-axis). Bottom: The most recent available Gini indices are shown for reference. Uganda is the only country with GDP and Gini index data available for approximately the same years as the surveys. Both metric values are provided by the World Bank [28,29].

comparison analysis, we linearly transform the RWI scores to their IWI equivalents in M3 denoted by iwi (Equation (1)) as both are highly correlated (i.e., Pearson’s correlation coefficients: 0.93 – 0.99 [17]).

$$iwi = \frac{(rwi - rwi_{min}) * (iwi_{max} - iwi_{min})}{(rwi_{max} - rwi_{min})} + iwi_{min} \quad (1)$$

M2: IWI inference model by Lee and Braithwaite 2022 [17] combines feature-based and image-based models to enhance each other’s performance. It uses two cross-validation approaches similar to M1: 5-fold cross-validation (basic CV) and leave-one-country-out cross-validation (leave-country-out). Initially, an XGBoost (eXtreme Gradient Boosting) algorithm is trained on 249 features (infrastructure, night-time luminosity, and population density) to predict IWI scores. Bayesian optimization is employed to tune the hyperparameters, selecting the best configuration for the training dataset. The XGBoost model’s predictions are then used to train a Convolutional Neural Network (CNN) model that outputs a probability distribution of socioeconomic status (rich, upper-middle class, lower-middle class, poor) for a 1-square-mile area. These probabilities are then fed back into the XGBoost model, creating a cycle where the models iteratively improve by providing better training data.

M3: IWI inference model by Espín-Noboa et al. 2023 [8] extracts 957 features from seven data sources. Each location is defined by the centroid of each place, using a default bounding-box width of 1 mile. Some features are also queried within 2, 5, and 10 Km to capture the original locations of the DHS clusters, similar to M2. Features include high-resolution satellite imagery, demographics, mobility networks, and mobile phone antennas. Three machine learning models are proposed to predict both the mean and standard deviation of IWI scores, providing insights into the wealth distribution within clusters. The first model is a CNN that predicts IWI scores from daylight satellite images. This CNN comprises 22 layers, with the final layer using a linear activation function and MSE as the loss function, tuning 4 hyperparameters. The second model is a

CatBoost regressor (CB), predicting IWI scores from 173 metadata features and evaluated individually for each data source. This model is tuned using 11 hyperparameters. The third model combines CNN+CB by feeding the third-to-last layer of the CNN into the CB model, adding 784 features. For training, data is partitioned into 80% train and 20% test sets, stratified into 10 equal-width bins of wealth. A 4-fold cross-validation on the train set, stratified by SES (ses CV), is used to tune hyperparameters via Random Search on 200 combinations. This process is repeated three times independently with different random seeds, to control for fluctuations, and mean performance is reported. The models are evaluated on various configurations of training data, including different years of ground-truth data, relocation strategies, data augmentation ($*_a$), sample weight strategies ($*_w$), and feature sources, ensuring robust and comprehensive performance evaluation. For our analysis, we chose the model with the best performance (lowest root-mean-square error, RMSE) in each country: CB for Sierra Leone and Liberia, CB_w for Uganda and Rwanda, and CNN_a+CB for Gabon and South Africa.

In summary, all models use a multi-modal and hybrid approach, combining features from various data sources and two model architectures, see Table 1 (bottom). M1 and M3 use satellite images by pre-training a CNN model and feeding the image embeddings into a gradient boosting algorithm. M2 also uses a hybrid approach but first pre-trains a gradient boosting algorithm to train a CNN, and then creates a feedback loop that enhances the initial model. Only M1 estimates the expected error of each location, though its explanatory power is limited (average $R^2 = 0.09$). All models predict the mean wealth of locations, but only M3 additionally predicts their standard deviation, and proposed two additional models to separate the effects of images and metadata.

2.3 Expected Trends

Before digging into the comparison of predictions between the three models of interest [2,17,8], it is crucial to acknowledge the discrepancies in the ground-truth data used to train them. Table 1 (top) outlines the specific years for which each approach utilized data for each country. This variation in time is significant because wealth and poverty are dynamic concepts that can fluctuate over time. To address this, rather than comparing directly the predicted values, we focus on the trends in predictions. We will achieve this by examining the trends of changes in Gross Domestic Product (GDP) per capita provided by the World Bank [28], as depicted in Figure 1 (top). By analyzing these trends, we can hypothesize that the comparison between RWI and IWI will mirror the trends observed in GDP. This approach allows us to account for potential discrepancies arising from the distinct time-frames of the datasets.

Additionally, we compare the changes in the heterogeneity of the predicted wealth distributions with each country’s official Gini index. Due to the lack of data from the World Bank [29], for the same years as the surveys in most countries, see Figure 1 (bottom), we present comparisons only for Uganda, where data is available, and South Africa, where all models used the same ground-truth.

Table 2: **Prediction statistics.** We show the number N of target locations contained in the inferred poverty maps, and the mean, standard deviation (SD), and Gini coefficient of the predicted wealth scores for each model. RWI scores are linearly transformed to their IWI equivalents, see Equation (1).

Country's Code	M1 ($I\hat{W}I$)				M2 (IWI)				M3 (IWI)			
	N	Mean	SD	Gini	N	Mean	SD	Gini	N	Mean	SD	Gini
SLE	8435	29.12	4.92	8.79	13040	18.93	10.34	23.01	9881	21.87	6.09	11.54
LBR	6189	28.62	3.71	6.72	16525	14.57	8.79	25.93	15597	23.35	3.74	7.75
UGA	25404	41.35	3.06	3.92	27482	22.27	11.26	25.09	27791	41.83	5.21	5.95
RWA	3715	45.81	2.93	3.38	23323	24.40	14.51	28.96	1150	47.79	3.46	3.74
ZAF	39072	48.95	8.59	9.69	22687	61.14	18.10	16.85	3043	52.65	14.11	15.04
GAB	1110	51.40	5.15	5.32	4835	21.89	8.86	17.93	1135	48.32	6.72	7.38

3 Results

Here, we compare the inferred poverty maps produced by M1, M2, and M3. We first present the predicted overall wealth distributions. Due to the lack of ground truth in all places of these poverty maps, we compare the predicted distributions with official GDP and Gini coefficient trends to understand how well these predictions align with established economic indicators. Given that each study employs different spatial resolutions, our comparison then focuses on locations that appear in all three studies. Note that these analyses are based on the predicted poverty maps rather than test sets with ground truth. We trained all variants of M3 models and use the best model in each country based on their lowest RMSE scores (see details in Section 2.2) to infer the final poverty maps. The inferences of all models are publicly available: M1 [19], M2 [16], and M3 [9]. For a comparison of the reported predictive power in terms of R^2 for these studies on their respective test sets, please refer to Appendix Table A1.

3.1 Predicted wealth distribution

Table 2 summarizes the poverty map inferences for each country and model. First, we observe that M2 generally identifies more locations (OSM populated places) than M1 and M3. Second, after re-scaling RWI scores for a fair comparison (see Equation (1)), we find that M2 predicts the lowest mean wealth in most cases, except in South Africa. In contrast, the mean wealth predicted by M1 and M3 between each country is very similar. Third, in terms of standard deviation (SD), M1 predicts a more homogeneous wealth distribution, characterized by lower values of SD and Gini coefficient. M3 follows, and M2 exhibits the highest SD and Gini coefficients, indicating greater wealth inequality in its predictions.

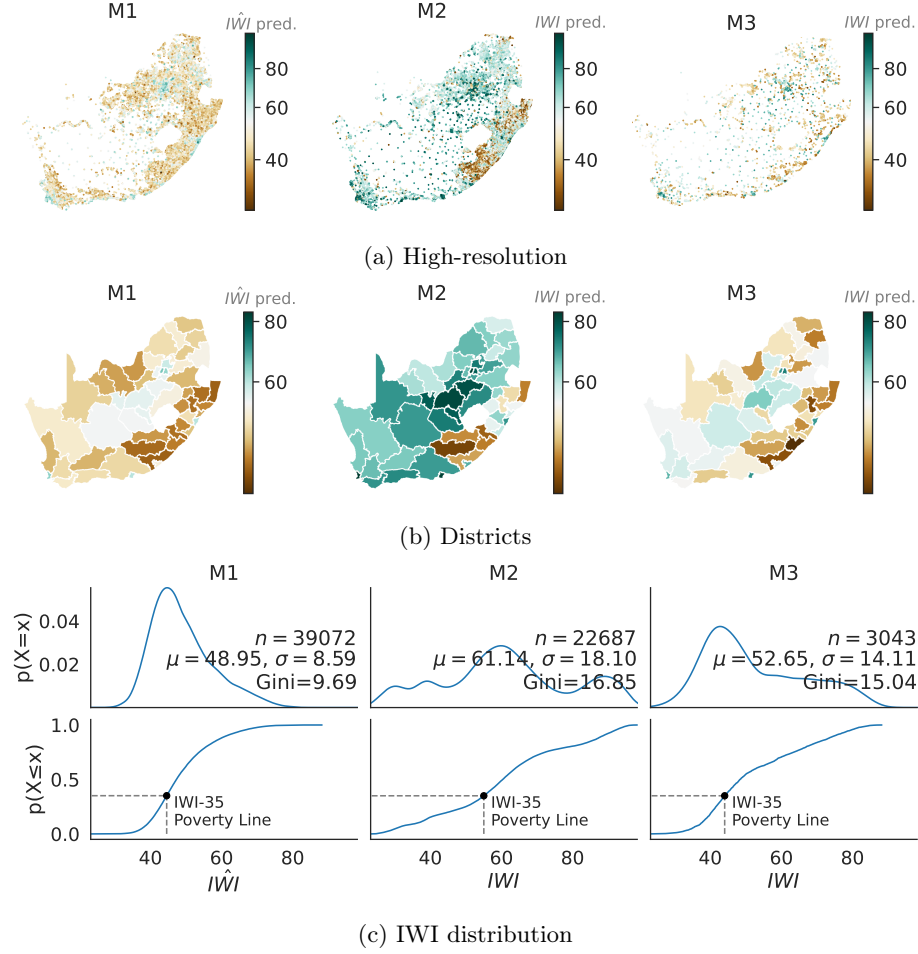


Fig. 2: IWI predictions in South Africa, ZAF (M3: CNN_a+CB). All models were trained on the same ground-truth data (2016), thus, we expect similar results. Color bars display the average predicted IWI scores, centered at the mean of M3's predictions for comparison. (a) Prediction at the original resolution, 2.4 km grid-cells (M1), and OSM populated places (M2, M3). Both M2 and M3 include the Marion Island, omitted here for visualization purposes. (b) Aggregated mean wealth at the district level (administrative level 2). Compared to M3, M2 predicts higher wealth, while M1 predicts slightly lower values. (c) Predicted wealth distribution (top: PDF, bottom: CDF). All subplots share the axis labels of the leftmost and bottom plots. ZAF is the second country with the highest GDP in our study (see Figure 1), and this is reflected in the prediction by all models (e.g., $\mu > 48$). Both M1 and M3 predict skewed, unimodal distributions of wealth, while M2 predicts an unusual multimodal distribution. IWI poverty line (35th percentile, corresponding to poverty headcount ratios at \$1.25 a day [23]) is the same between M1 and M3, but differs for M2.

Table 3: **Expected vs. obtained differences in wealth.** The direction of change in wealth between M1 and M3 generally aligns with World Bank GDP trends, especially in SLE, LBR, UGA, RWA, and GAB. In contrast, the direction of change in wealth between M2 and M3 is only observed in RWA, with larger than expected differences. Most comparisons are significantly different ($p < 0.001$, using a two-sample KS-test [11]), except in SLE for M1 and M3. **Highlighted values** accurately capture the expected trend’s sign (+/-).

Country’s Code	M1 ($I\hat{W}I$) vs. M3 (IWI)					M2 (IWI) vs. M3 (IWI)				
	Exp. IWI	Obt. IWI	Exp. Gini	Obt. Gini	KS	Exp. IWI	Obt. IWI	Exp. Gini	Obt. Gini	KS
SLE	0.16	0.14	NA	-2.75	0.74	0.01	-0.07	NA	11.47	0.62 ***
LBR	0.04	0.10	NA	-1.02	0.67 ***	0.04	-0.23	NA	18.19	0.83 ***
UGA	-0.04	-0.01	-1.7	-2.02	0.13 ***	0.0	-0.31	0.0	19.15	0.87 ***
RWA	-0.05	-0.02	NA	-0.36	0.34 ***	-0.05	-0.32	NA	25.22	0.85 ***
ZAF	0.00	-0.04	0.0	-5.34	0.18 ***	0.0	0.07	0.0	1.81	0.30 ***
GAB	0.11	0.03	NA	-2.06	0.45 ***	NA	-0.38	NA	10.55	0.95 ***

Expected IWI Difference = $(GDP_{Y_{M*}} - GDP_{Y_{M3}})/(GDP_{Y_{M*}} + GDP_{Y_{M3}})$

Obtained IWI Difference = $(\mu_{IWI_{M*}} - \mu_{IWI_{M3}})/(\mu_{IWI_{M*}} + \mu_{IWI_{M3}})$

Expected Gini Difference = $(Gini_{Y_{M*}} - Gini_{Y_{M3}})$

Obtained Gini Difference = $(Gini_{M*} - Gini_{M3})$

Here, M^* represents either M1 or M2, respectively. Y_{M^*} denotes the year of the ground-truth data used to train model M^* , which is then used to select the corresponding indicator, GDP per capita or Gini coefficient, from the World Bank.

3.2 Expected vs. Obtained Trends

We compared M1 and M2 to M3, focusing on their expected performance based on changes in GDP per capita per country over the years of each model’s data.⁴ Results are shown in Table 3. In Uganda, where M2 and M3 used the same ground-truth, we expect similar wealth predictions. However, M2 inferred lower and more heterogeneous wealth than M3. In South Africa, despite all models using the same ground-truth data, we found differing results: M1 predicted slightly lower wealth values than M3, and M2 predicted slightly higher values. These patterns are visualized in Figure 2 (Appendix A.2 for other countries). In Liberia, models M1, M2, and M3 used ground-truth data from 2013, 2016, and 2019/2022, respectively (Table 1). During this period, GDP per capita rose from 717.6 in 2013 to 722.1 in 2016, dropped to 665.9 in 2019, and increased to 754.5 in 2022 (Figure 1). The normalized GDP difference between 2013 and 2019 (0.04) suggests that M3’s IWI scores should be slightly lower than M1’s, and that is what we obtained (0.1). However, even though the same trend was expected between M2 and M3, M2’s IWI scores were unexpectedly lower (-0.23). In terms of Gini

⁴ Since M3 is used as a baseline for comparison with both M1 and M2, comparing M1 and M2 directly is unnecessary because their relative performance can be inferred from their respective comparisons to M3.

Table 4: **Prediction differences in overlapping locations.** Due to the differing spatial resolutions between the models (grid-cells vs. OSM populated places), we compare predictions only for overlapping locations. We spatially joined locations from M1 and M3, and M2 and M3, defining overlap as places in study i that are also in study j within a distance of less than 500 m . As expected, M3 contains more overlapping locations N_o with M2 than with M1, since both M2 and M3 use OSM populated places. Although M2’s predictions are more positively correlated with M3’s, M3’s predictions are closer to M1’s (low RMSE) than to M2’s (high RMSE), consistent with the overall distributions (Table 2). **Highlighted values** accurately capture the expected trend’s sign (+/-)

Country’s Code	M1 ($I\hat{W}I$) vs. M3 (IWI)					M2 (IWI) vs. M3 (IWI)				
	N_o	RMSE	Pearson Corr.	IWI Diff.	Gini Diff.	N_o	RMSE	Pearson Corr.	IWI Diff.	Gini Diff.
SLE	1125	9.72	0.69 ***	-0.16	-1.08	7264	6.89	0.87 ***	0.08	10.34
LBR	1332	6.59	0.53 ***	-0.11	-0.51	14609	11.06	0.74 ***	0.26	15.66
UGA	2799	3.69	0.73 ***	-0.02	0.06	13057	19.58	0.82 ***	0.26	20.47
RWA	95	4.63	0.25 *	-0.01	0.27	1603	21.77	0.43 ***	0.20	21.19
ZAF	314	12.98	0.59 ***	-0.04	-6.02	2866	22.78	0.45 ***	-0.13	0.52
GAB	43	6.47	0.62 ***	-0.03	-3.29	598	25.21	0.73 ***	0.32	18.06

$$\text{IWI Difference} = (\mu_{IWI_{M^*}} - \mu_{IWI_{M3}}) / (\mu_{IWI_{M^*}} + \mu_{IWI_{M3}})$$

$$\text{Gini Difference} = (Gini_{M^*} - Gini_{M3})$$

coefficients, M3 generally predicted more heterogeneous IWI scores than M1 and more homogeneous scores than M2. In Uganda, M2 indicated greater inequality than M3 (19.15), which in turn showed more inequality than M1 (−2.02). The same pattern was observed in South Africa, although the same poverty skewness was expected across models. Due to data limitations, we were unable to track Gini coefficient trends for the other countries.

3.3 Overlapping locations

The previous results compared the overall predictions across all models, providing a general understanding of their performance relative to country-level GDP per capita and Gini coefficient trends. Now, we focus on comparing the predictions for locations that overlap in all three studies. It is important to note that the three studies differ in the spatial resolution of their poverty maps: M1 uses grid cells, while M2 and M3 use OSM populated places (see details in Section 2.1). Therefore, we perform a spatial join to analyze only these overlapping locations, which we expect to perfectly reflect the anticipated trends.

As before, we use M3 as a baseline model to compare the differences across all models, with results presented in Table 4. Unexpectedly, the observed trends are not consistently maintained across most countries and models. Notable exceptions include Uganda and Rwanda, where M3 infers higher mean wealth than

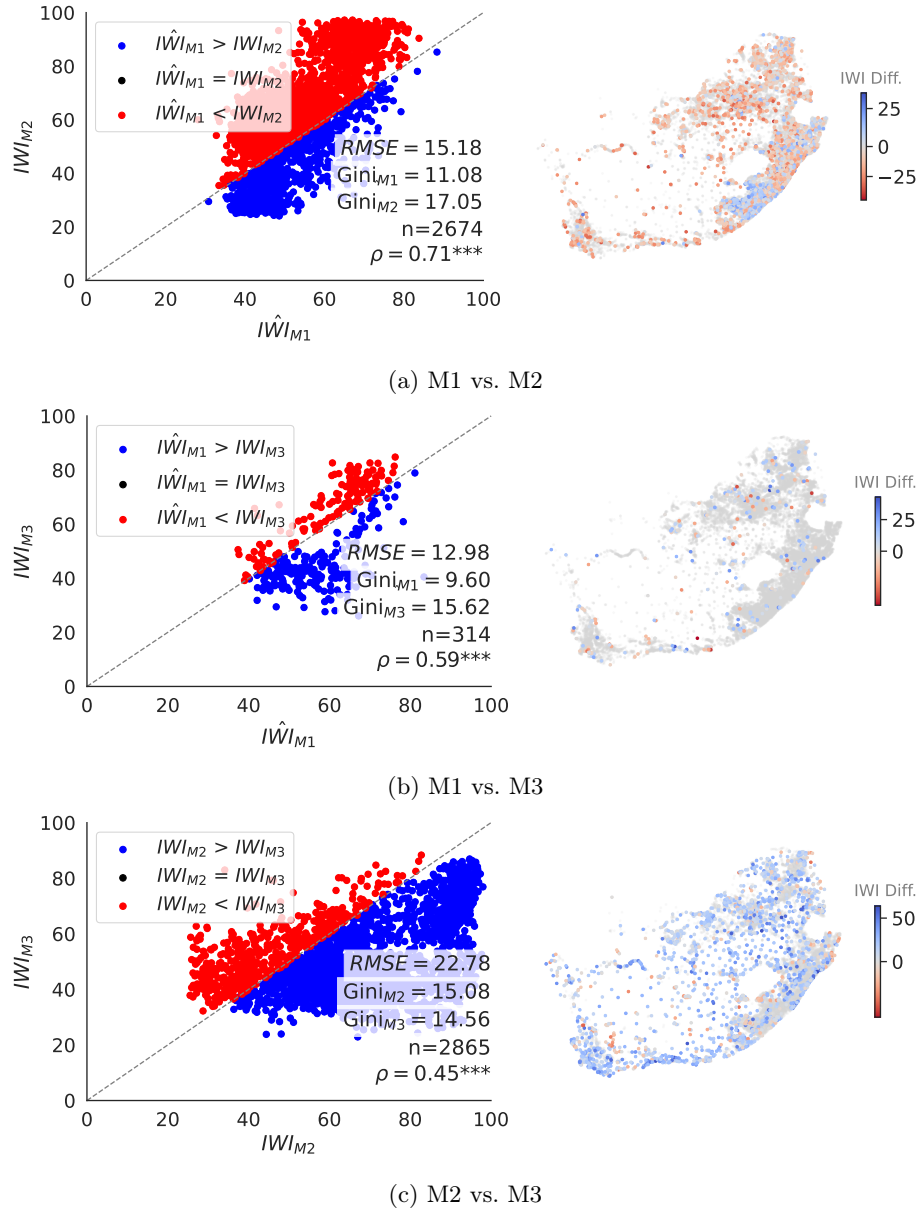


Fig. 3: IWI predictions at overlapping locations in South Africa, ZAF (M3: CNN_a+CB). Right: IWI differences between the predictions of two models for each overlapping location. Left: Correlation between these predictions. Colors indicate the direction of the differences per model pair: (a) M1 vs. M2, (b) M1 vs. M3, and (c) M2 vs. M3. M2 generally overestimates wealth compared to M1 (mostly red in (a)) and M3 (mostly blue in (c)). Moreover, the wealth distribution in these locations is equally skewed. In (b), M1's predictions are more homogeneous than M3's, despite achieving relatively low RMSE.

M1, and Sierra Leone and Liberia, where M3 infers lower mean wealth than M2, aligning with the expected GDP trends over time (see Table 3). In the specific case of South Africa, where all models were trained using the same ground truth data, M3’s mean wealth in these overlapping locations is higher than that inferred by the other models. Nevertheless, M2’s heterogeneity is closer to that M3, while M1 produced more homogeneous wealth scores, see Figure 3 (Appendix A.3 for other countries).

4 Conclusions

To assess the alignment between the IWI score predictions by three models—M1 (Chi et al., 2022 [2]), M2 (Lee and Braithwaite, 2022 [17]), and M3 (Espín-Noboa et al., 2023 [8])—we examined the differences in their underlying ground-truth data and compared predicted wealth trends against expected changes in GDP per capita. Overall, the differences between M1 and M3 generally met expectations. Sierra Leone, Liberia, and Gabon showed higher mean wealth in M1 compared to M3, while South Africa showed lower values, and Uganda and Rwanda had similar ones. Small differences suggested stable wealth in Uganda, Rwanda, South Africa, and Gabon over time (M1 \rightarrow M3). However, M2’s predictions did not align as expected, indicating lower poverty levels in several countries, except in South Africa, where M2’s IWI scores were slightly higher than M3’s. In general, the wealth distribution predicted by M3 was slightly more heterogeneous than that inferred by M1, but more homogeneous compared to M2. These trends were particularly observed in Uganda (as expected) when comparing M1 and M3, and in both South Africa and Uganda when comparing M2 with M3, although we anticipated the wealth distributions to be equally skewed between these two models in these two countries.

When comparing the trends in the locations that appear in all three studies (i.e., overlaps), the expected trends were not consistently observed in most countries. Nevertheless, predictions by M1 are the closest to those by M3 compared to M2, particularly in Uganda, Rwanda, South Africa and Gabon. Similar to the overall distributions, M2’s predictions for this set of places produce the most heterogeneous wealth distribution (i.e., highest inequality). Given the lack of official Gini coefficients for the years of interest for most countries, we cannot evaluate whether these trends in heterogeneity are expected. However, in South Africa, we anticipated minimal differences as all models use the same ground truth data. Only M2 and M3 reflect this expected trend.

These findings indicate that the predictions by Chi et al. and Espín-Noboa et al. align with general GDP trends over time. Differences in their predictions are expected since each study used data from different periods. For instance, Sierra Leone’s GDP decline from 2013 to 2016 and 2019 (Figure 1) is reflected in the corresponding drop in IWI (re-scaled RWI) (2013) and IWI (2016, 2019) scores (Table 2). Discrepancies with the overall predictions by Lee and Braithwaite, as well as among the overlapping locations, underscore the necessity for policymakers and African stakeholders to further audit these models and predicted maps

to ensure their validity before deployment. While evaluations during training are important, they are insufficient to capture the overall validity of the inferred wealth indicators, as they subjectively focus on the model’s performance on the test data. Accurate poverty maps are essential for effective policy interventions and play a crucial role in addressing the United Nations’ first sustainable development goal: eradicating poverty world-wide.

Acknowledgments. This work was funded by the SoBigData++ project (H2020-871042), Dataredux ANR project (ANR-19-CE46-0008), and the CHIST-ERA project SAI: FWFI 5205-N. The presented computational results have been achieved in part using the Vienna Scientific Cluster (VSC). This work was partially funded by the Vienna Science and Technology Fund WWTF under project No. ICT20-079. We thank the Data for Good team at Meta for insightful discussions during the first partner lightning talks, where early versions of this work were presented. We also appreciate the authors of the analyzed papers for their open data practices, which made this audit possible.

Disclosure of Interests. The authors have no competing interests to declare that are relevant to the content of this article.

References

1. Burgert, C.R., Colston, J., Roy, T., Zachary, B.: Geographic displacement procedure and georeferenced data release policy for the Demographic and Health Surveys. Icf International (2013)
2. Chi, G., Fang, H., Chatterjee, S., Blumenstock, J.E.: Microestimates of wealth for all low-and middle-income countries. *Proceedings of the National Academy of Sciences* **119**(3), e2113658119 (2022)
3. Córdova, A.: Methodological note: Measuring relative wealth using household asset indicators. *AmericasBarometer Insights* **6**(1), 1–9 (2009)
4. Cruz, E., Vaca, C., Villavicencio, M.: Estimating urban socioeconomic inequalities through airtime top-up transactions data. In: 2021 IEEE International Conference on Big Data (Big Data). pp. 4265–4272. IEEE (2021)
5. Data for Good by Facebook: Relative Wealth Index (2024), <https://dataforgood.facebook.com/dfg/tools/relative-wealth-index>, accessed: 2024-08-01
6. Dong, Y., Yang, Y., Tang, J., Yang, Y., Chawla, N.V.: Inferring user demographics and social strategies in mobile social networks. In: *Proceedings of the 20th ACM SIGKDD international conference on Knowledge discovery and data mining*. pp. 15–24 (2014)
7. Ebener, S., Murray, C., Tandon, A., Elvidge, C.C.: From wealth to health: modelling the distribution of income per capita at the sub-national level using night-time light imagery. *international Journal of health geographics* **4**, 1–17 (2005)
8. Espín-Noboa, L., Kertész, J., Karsai, M.: Interpreting wealth distribution via poverty map inference using multimodal data. In: *Proceedings of the ACM Web Conference 2023*. pp. 4029–4040 (2023)
9. Espín-Noboa, L.: Poverty Maps (2023), <https://github.com/lisette-espín/PovertyMaps>
10. Ghosh, T., L Powell, R., D Elvidge, C., E Baugh, K., C Sutton, P., Anderson, S.: Shedding light on the global distribution of economic activity. *The Open Geography Journal* **3**(1) (2010)

11. Hodges Jr, J.: The significance probability of the smirnov two-sample test. *Arkiv för matematik* **3**(5), 469–486 (1958)
12. Hotelling, H.: Analysis of a complex of statistical variables into principal components. *Journal of educational psychology* **24**(6), 417 (1933)
13. ICF International: The Demographic and Health Surveys (DHS) Program (2024), <https://dhsprogram.com>, accessed: 2024-08-01
14. Jean, N., Burke, M., Xie, M., Davis, W.M., Lobell, D.B., Ermon, S.: Combining satellite imagery and machine learning to predict poverty. *Science* **353**(6301), 790–794 (2016)
15. Jolliffe, I.T., Cadima, J.: Principal component analysis: a review and recent developments. *Philosophical transactions of the royal society A: Mathematical, Physical and Engineering Sciences* **374**(2065), 20150202 (2016)
16. Lee, K.: High-resolution poverty maps in Sub-Saharan Africa (2022). <https://doi.org/10.7910/DVN/50GWYM>
17. Lee, K., Braithwaite, J.: High-resolution poverty maps in sub-saharan africa. *World Development* **159**, 106028 (2022)
18. Levy, A.J., Karsai, M., Fleury, E.: Optimal proxy selection for socioeconomic status inference on twitter. *Complexity* **2019**, 6059673–6059673 (2019)
19. Meta: Relative Wealth Index (2023), <https://data.humdata.org/dataset/relative-wealth-index>
20. Piaggese, S., Giurgola, S., Karsai, M., Mejova, Y., Panisson, A., Tizzoni, M.: Mapping urban socioeconomic inequalities in developing countries through facebook advertising data. *Frontiers in big Data* **5**, 1006352 (2022)
21. Poirier, M.J., Grépin, K.A., Grignon, M.: Approaches and alternatives to the wealth index to measure socioeconomic status using survey data: a critical interpretive synthesis. *Social Indicators Research* **148**(1), 1–46 (2020)
22. Serajuddin, U., Uematsu, H., Wieser, C., Yoshida, N., Dabalen, A.: Data deprivation: another deprivation to end. *World Bank policy research working paper* (7252) (2015)
23. Smits, J., Steendijk, R.: The international wealth index (iwi). *Social indicators research* **122**, 65–85 (2015)
24. The DHS Program: Wealth index (2024), <https://dhsprogram.com/topics/wealth-index/>, accessed: 2024-08-01
25. Uganda Bureau of Statistics: The Uganda Poverty Map Report. Tech. rep. (October 2019), https://www.ubos.org/wp-content/uploads/publications/02_2020Poverty_Map_report__Oct_2019.pdf, accessed: 2024-07-31
26. United Nations: Sustainable Development Goal 1: No Poverty. <https://sdgs.un.org/goals/goal1> (2015), accessed: 2024-07-31
27. Wang, P.Y., Chen, C.T., Su, J.W., Wang, T.Y., Huang, S.H.: Deep learning model for house price prediction using heterogeneous data analysis along with joint self-attention mechanism. *IEEE Access* **9**, 55244–55259 (2021)
28. World Bank: GDP per capita (current US\$) (2024), <https://data.worldbank.org/indicator/NY.GDP.PCAP.CD>, accessed: 2024-08-01
29. World Bank: Poverty and Inequality Platform. Gini index. For more information and methodology, please see <https://pip.worldbank.org>. (2024), <https://data.worldbank.org/indicator/SI.POV.GINI>, accessed: 2024-08-01

A Appendix

In this appendix, we present the comparison of the three models, M1, M2, and M3, across the remaining five African countries considered in this study: Sierra Leone, Liberia, Uganda, Rwanda, and Gabon. This analysis supplements our main findings by providing additional insights into the performance and predictions of each model, highlighting the differences in wealth estimates.

Prediction data. Openly available here: M1 [19], M2 [16], and M3 [9].

A.1 Performance on test sets

Table A1: **Reported validation R^2 scores for each approach.** M1 reports validation results on census data, as shown in Fig. S4 of the supplementary information [2]. M2 presents validation results for single-country training in Table 1 [17]. We retrain the M3 models for each country using a subset of the original features reported in [8], and report the performance (R^2) of the best model, indicated by the lowest root-mean-square error, RMSE (see details in Section 2.2).

Country (Code) / R^2	M1	M2	M3
Sierra Leone (SLE)	83.0	89.82	80.7
Liberia (LBR)	-	89.3	76.3
Uganda (UGA)	-	89.02	78.5
Rwanda (RWA)	82.0	87.41	67.5
South Africa (ZAF)	-	73.03	49.5
Gabon (GAB)	-	-	81.9

A.2 Overall predictions

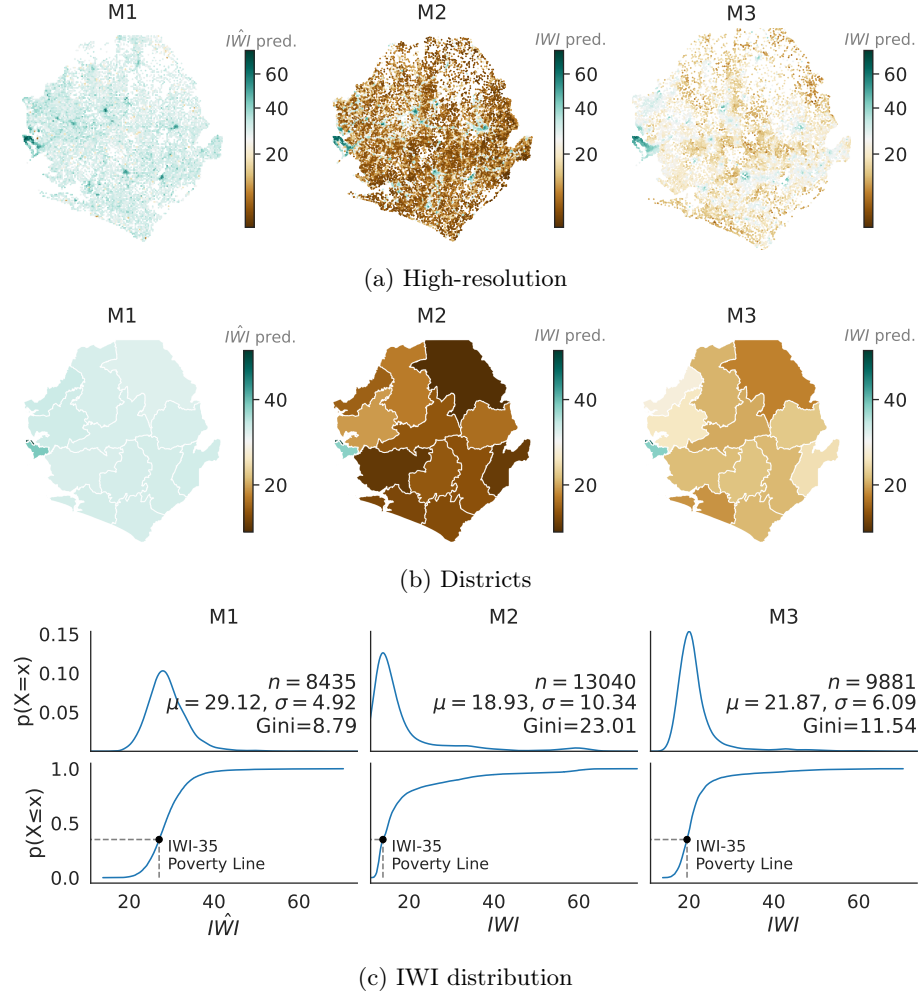


Fig. A1: **IWI predictions in Sierra Leone, SLE (M3: CB)**. We expect M1 and M2 to produce wealthier maps than M3 (Table 3), with M1 being the wealthiest (Table 2). Color bars display the average predicted IWI scores, centered at the mean of M3’s predictions for comparison. (a) Prediction at the original resolution. (b) Aggregated mean wealth at the administrative level 2. Compared to M3, M2 is consistently predicting lower wealth, while M1 predicts higher values (M1 and M3 fulfill the expectation). (c) Predicted wealth distribution (From top: PDF, CDF). All subplots share the axis labels of the leftmost and bottom plots. IWI poverty line (35th percentile, corresponding to poverty headcount ratios at \$1.25 a day [23]) varies across models, with M2 being slightly closer to M3.

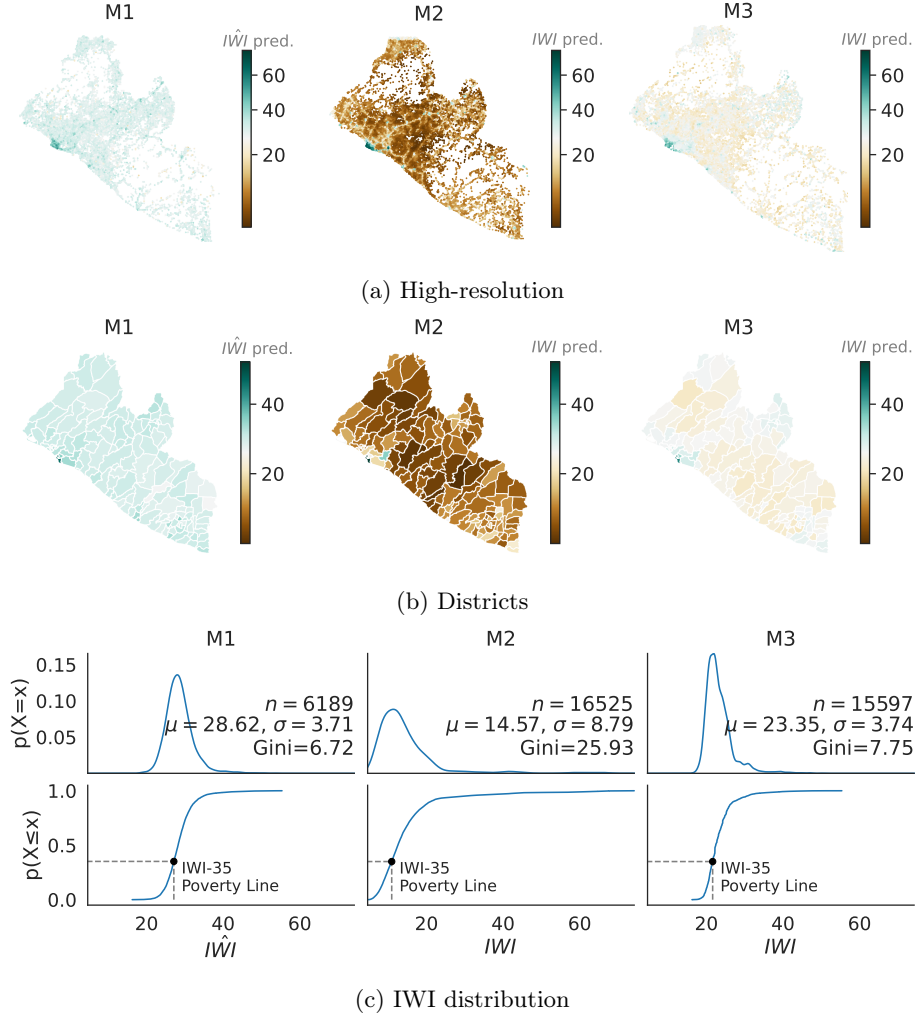


Fig. A2: **IWI predictions in Liberia, LBR (M3: CB)**. We expect both M1 and M2 to produce slightly wealthier maps than M3 (Table 3). Color bars display the average predicted IWI scores, centered at the mean of M3's predictions for comparison. (a) Prediction at the original resolution. (b) Aggregated mean wealth at the administrative level 2. Compared to M3, M2 is consistently predicting lower wealth, while M1 predicts higher values (M1 and M3 fulfill the expectation). (c) Predicted wealth distribution (From top: PDF, CDF). All subplots share the axis labels of the leftmost and bottom plots. IWI poverty line (35th percentile, corresponding to poverty headcount ratios at \$1.25 a day [23]) varies across models, with M1 being closer to M3.

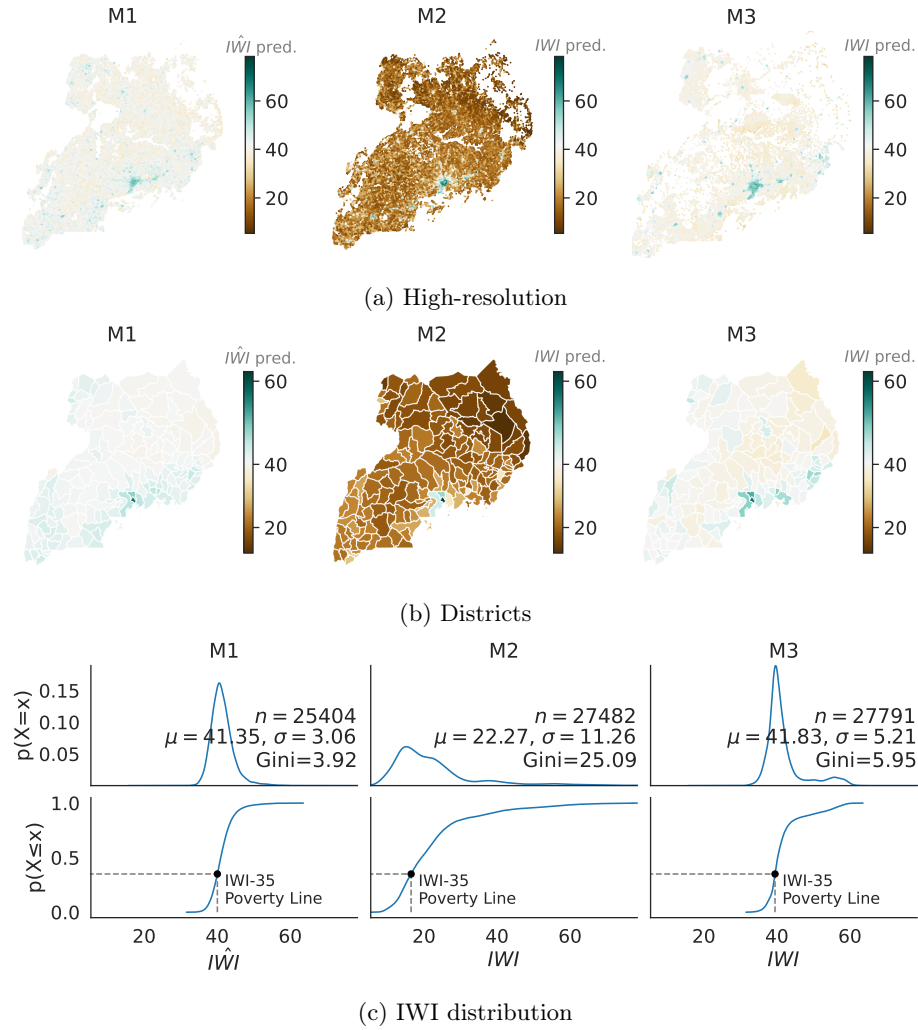


Fig. A3: **IWI predictions in Uganda, UGA (M3: CB_w)**. We expect M3 to produce slightly wealthier maps than M1 and comparable to M2 (Table 3). Color bars display the average predicted IWI scores, centered at the mean of M3's predictions for comparison. (a) Prediction at the original resolution. (b) Aggregated mean wealth at the administrative level 2. Compared to M3, M2 is consistently predicting lower wealth, while M1 predicts slightly lower values (M1 and M3 fulfill the expectation). (c) Predicted wealth distribution (From top: PDF, CDF). All subplots share the axis labels of the leftmost and bottom plots. IWI poverty line (35th percentile, corresponding to poverty headcount ratios at \$1.25 a day [23]) is the same between M1 and M3, but differs for M2.

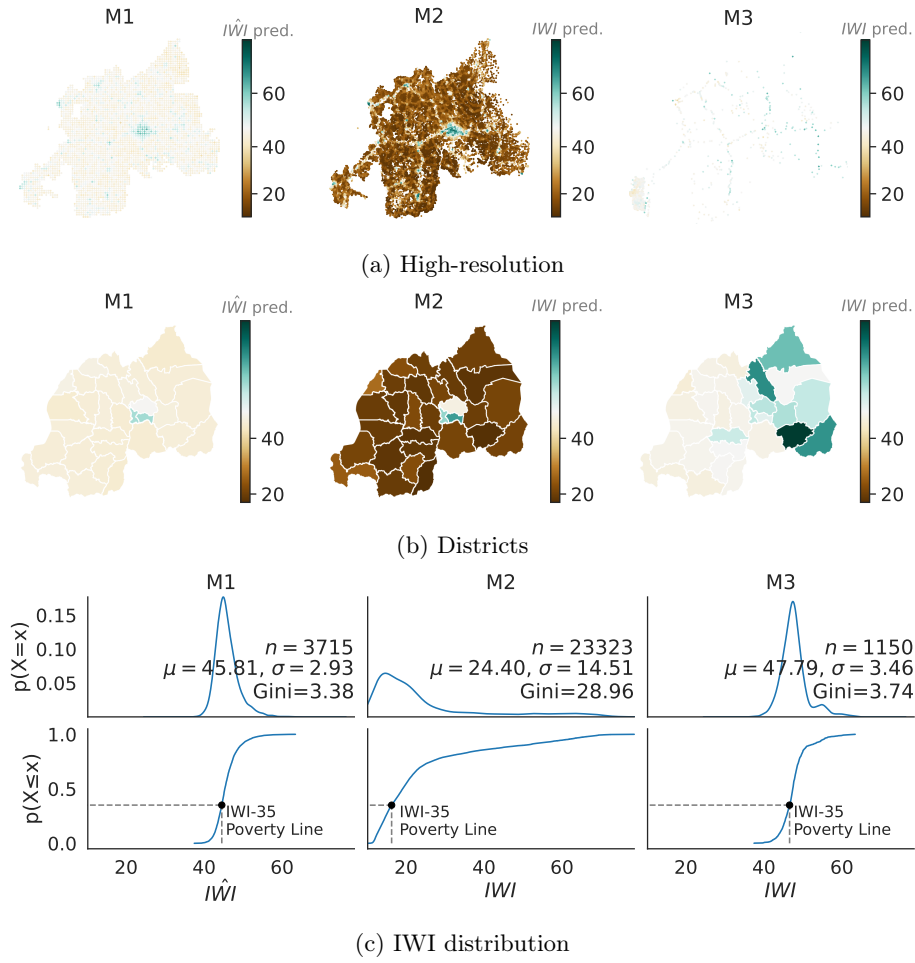


Fig. A4: **IWI predictions in Rwanda, RWA (M3: CB_w)**. We expect both M1 and M2 to produce slightly poorer poverty maps than M3 (Table 3). Color bars display the average predicted IWI scores, centered at the mean of M3's predictions for comparison. (a) Prediction at the original resolution. (b) Aggregated mean wealth at the administrative level 2. Compared to M3, both M2 and M1 predict lower wealth values. However, M2 is twice as poor than M1 (M1 and M3 fulfill the expectation). (c) Predicted wealth distribution (From top: PDF, CDF). All subplots share the axis labels of the leftmost and bottom plots. IWI poverty line (35th percentile, corresponding to poverty headcount ratios at \$1.25 a day [23]) varies across models, with M1 being closer to M3.

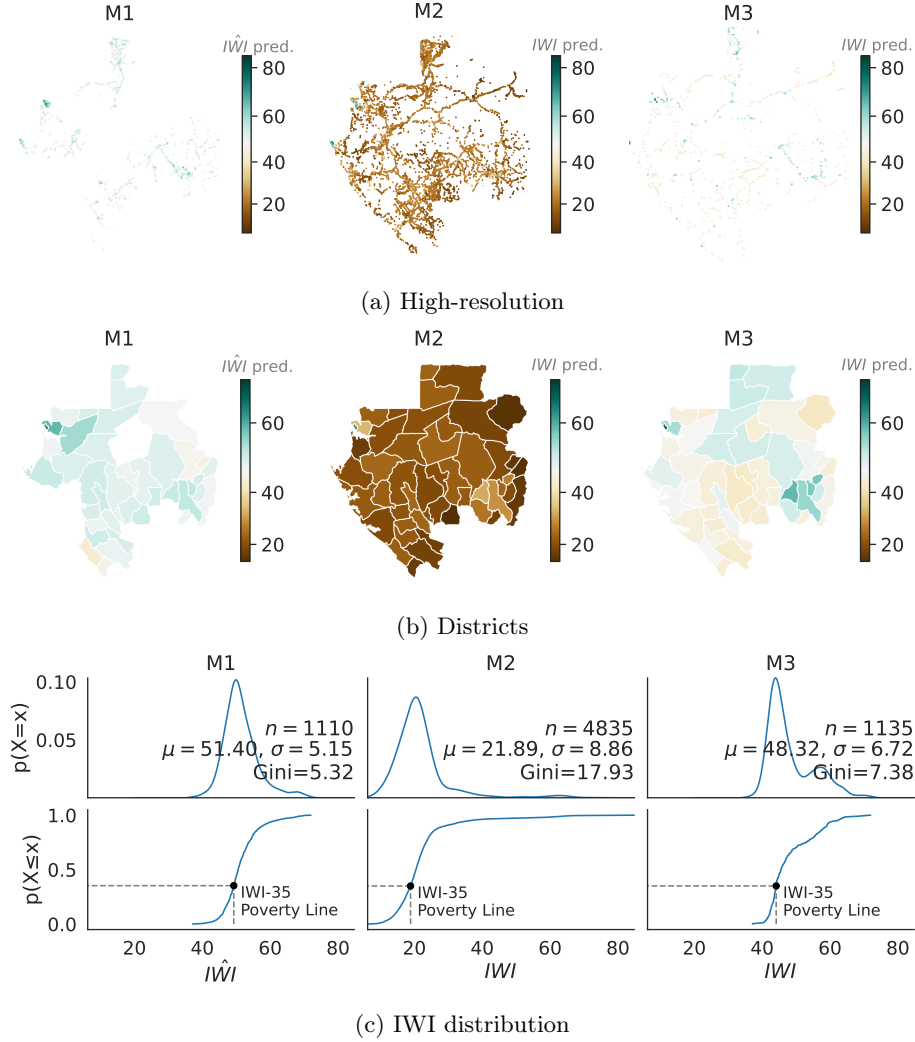


Fig. A5: **IWI predictions in Gabon, GAB (M3: CNN_a+CB)**. We expect M1’s poverty map to be wealthier than M3 (Table 3). Color bars display the average predicted IWI scores, centered at the mean of M3’s predictions for comparison. (a) Prediction at the original resolution. (b) Aggregated mean wealth at the administrative level 2. Compared to M3, M1 predicts a wealthier country (as expected). (c) Predicted wealth distribution (From top: PDF, CDF). All subplots share the axis labels of the leftmost and bottom plots. IWI poverty line (35th percentile, corresponding to poverty headcount ratios at \$1.25 a day [23]) varies across models, with M1 being closer to M3.

A.3 Overlapping locations

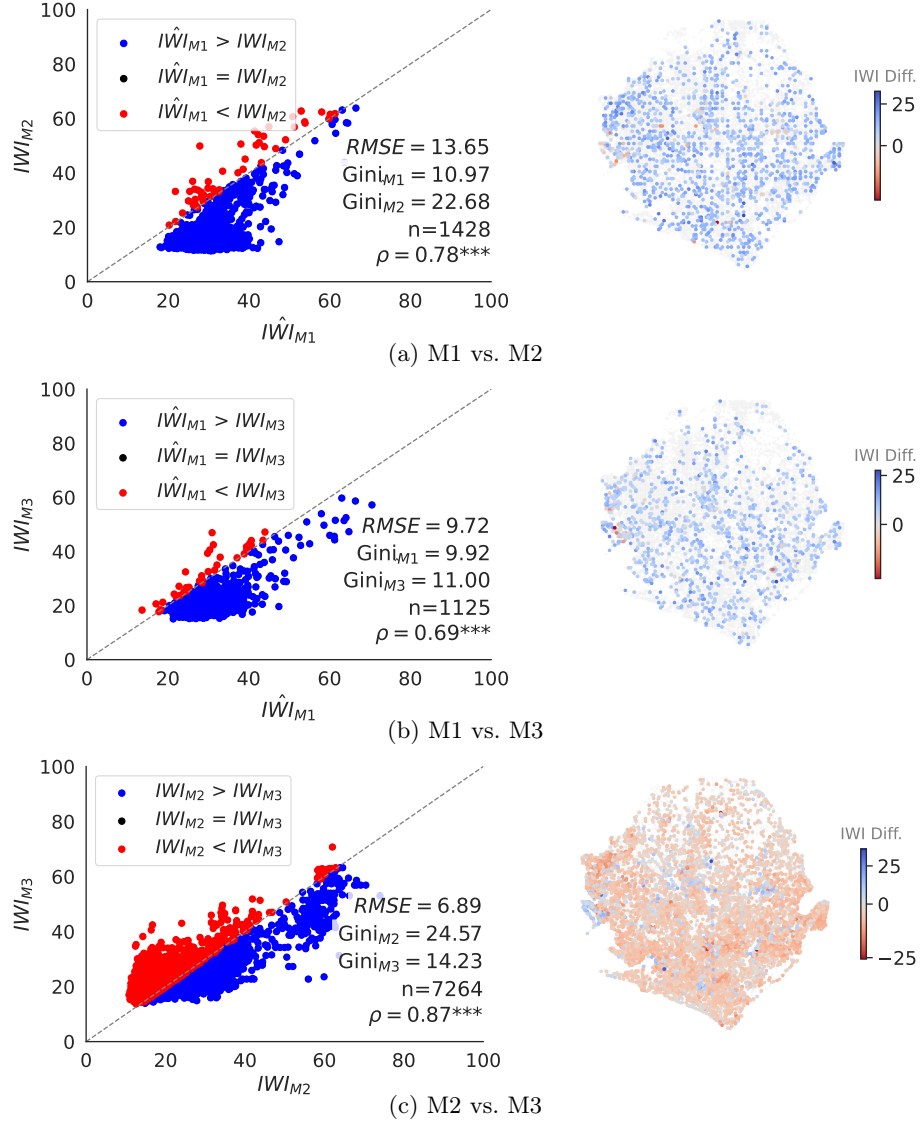


Fig. A6: **IWI predictions in overlapping locations in Sierra Leone, SLE (M3: CB).** Right: IWI differences between the predictions of two models for each overlapping location. Left: Correlation between these predictions. Colors indicate the direction of the differences. M1 generally overestimates wealth compared to M2 (blue in (a)) and M3 (blue in (b)), and predictions are more homogeneous. In (c), M2's predictions are more heterogeneous than M3's, despite achieving relatively low RMSE.

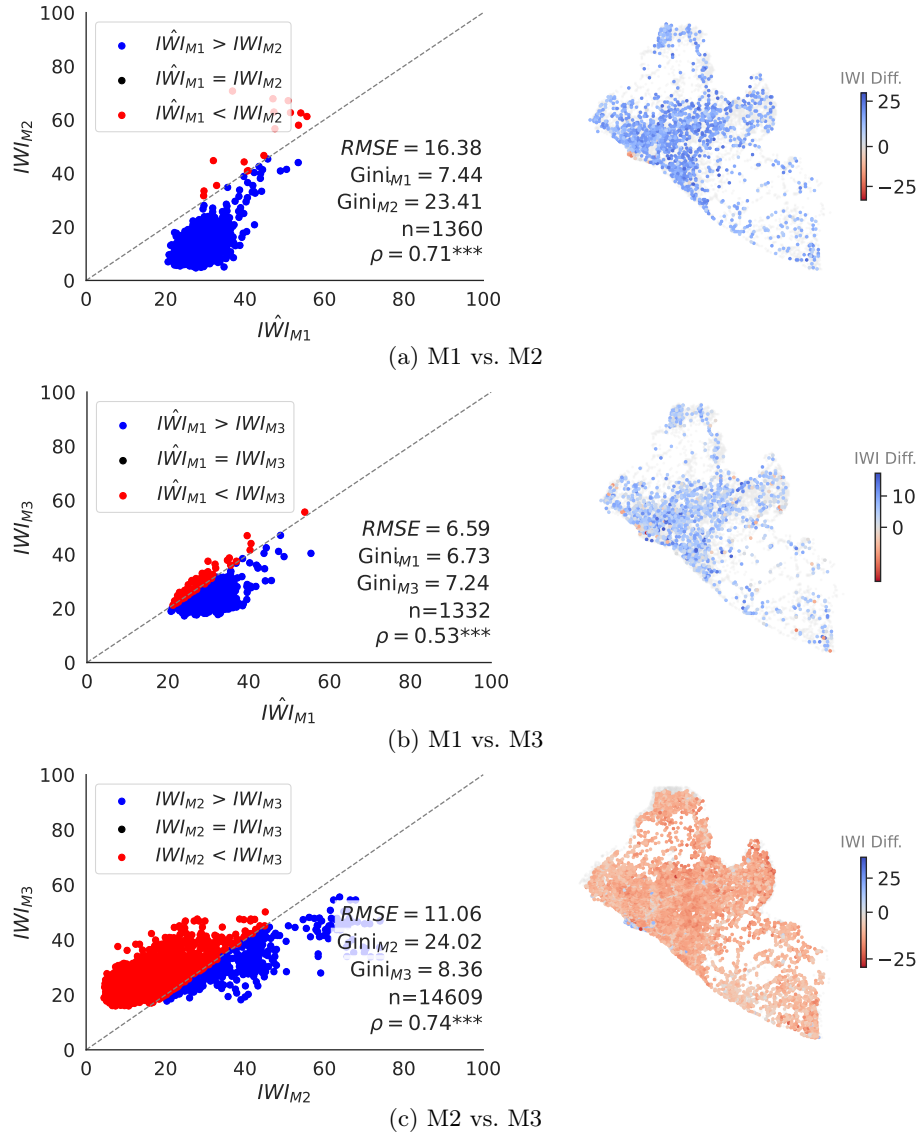


Fig. A7: **IWI predictions in overlapping locations in Liberia, LBR (M3: CB).** Right: IWI differences between the predictions of two models for each overlapping location. Left: Correlation between these predictions. Colors indicate the direction of the differences. M1 generally overestimates wealth compared to M2 (blue in (a)) and M3 (blue in (b)), and predictions are more homogeneous. In (c), M2's predictions are more heterogeneous than M3's.

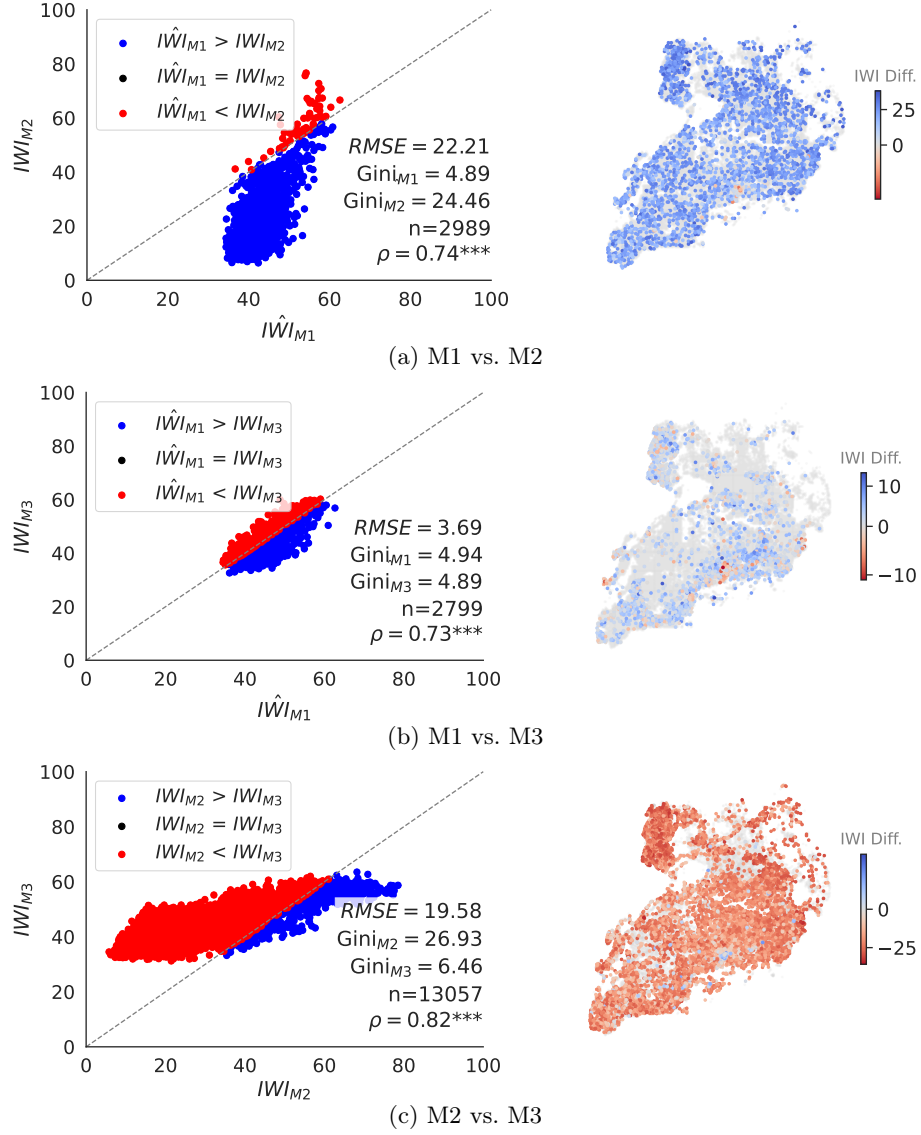


Fig. A8: **IWI predictions in overlapping locations in Uganda, UGA (M3: CB_w)**. Right: IWI differences between the predictions of two models for each overlapping location. Left: Correlation between these predictions. Colors indicate the direction of the differences. M1 generally overestimates wealth compared to M2 (blue in (a)) and M3 (blue in (b)). Predictions from M1 are more homogeneous than M2 and equally skewed as M3. In (c), M2's predictions are more heterogeneous than M3's.

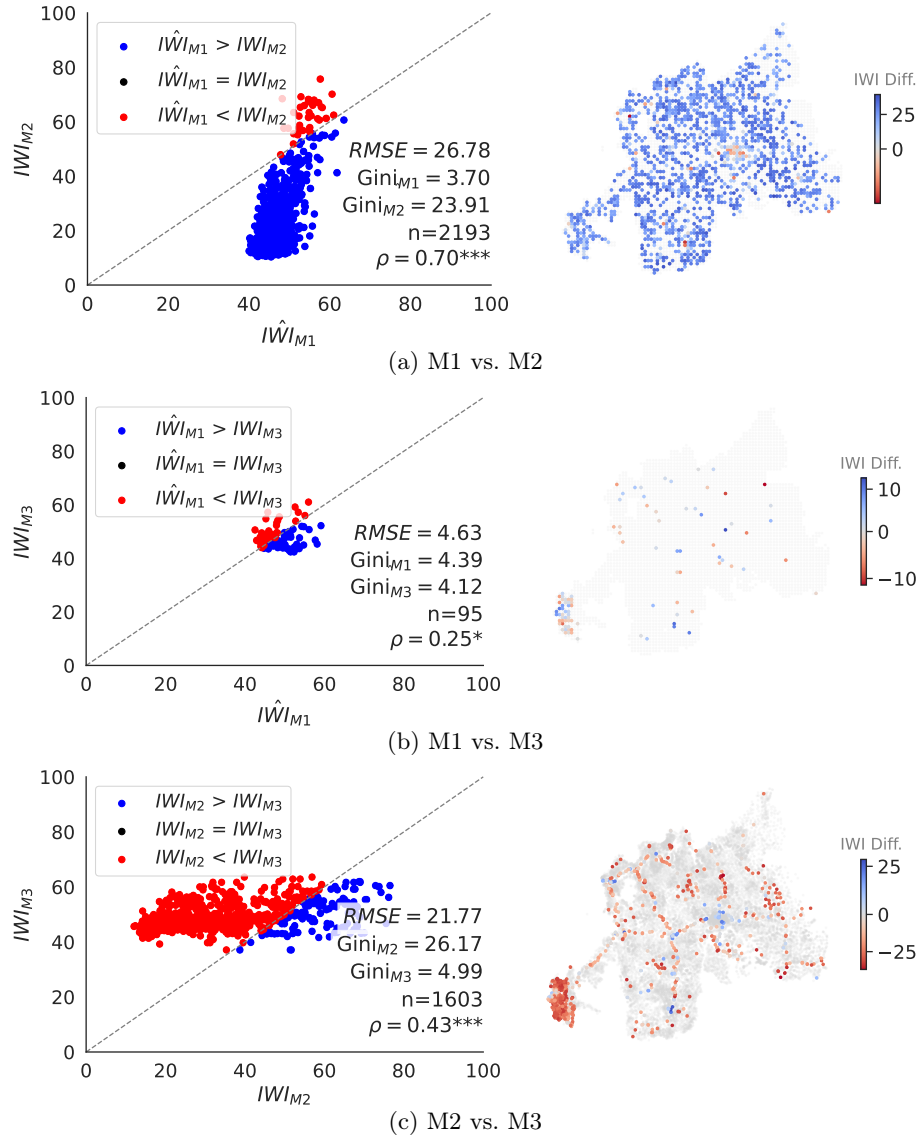


Fig. A9: **IWI predictions in overlapping locations in Rwanda, RWA (M3: CB_w)**. Right: IWI differences between the predictions of two models for each overlapping location. Left: Correlation between these predictions. Colors indicate the direction of the differences. M2 generally underestimates wealth compared to M1 (blue in (a)) and M3 (red in (c)). Predictions from M1 are more homogeneous than M2 and equally skewed as M3. In (c), M2's predictions are more heterogeneous than M3's.

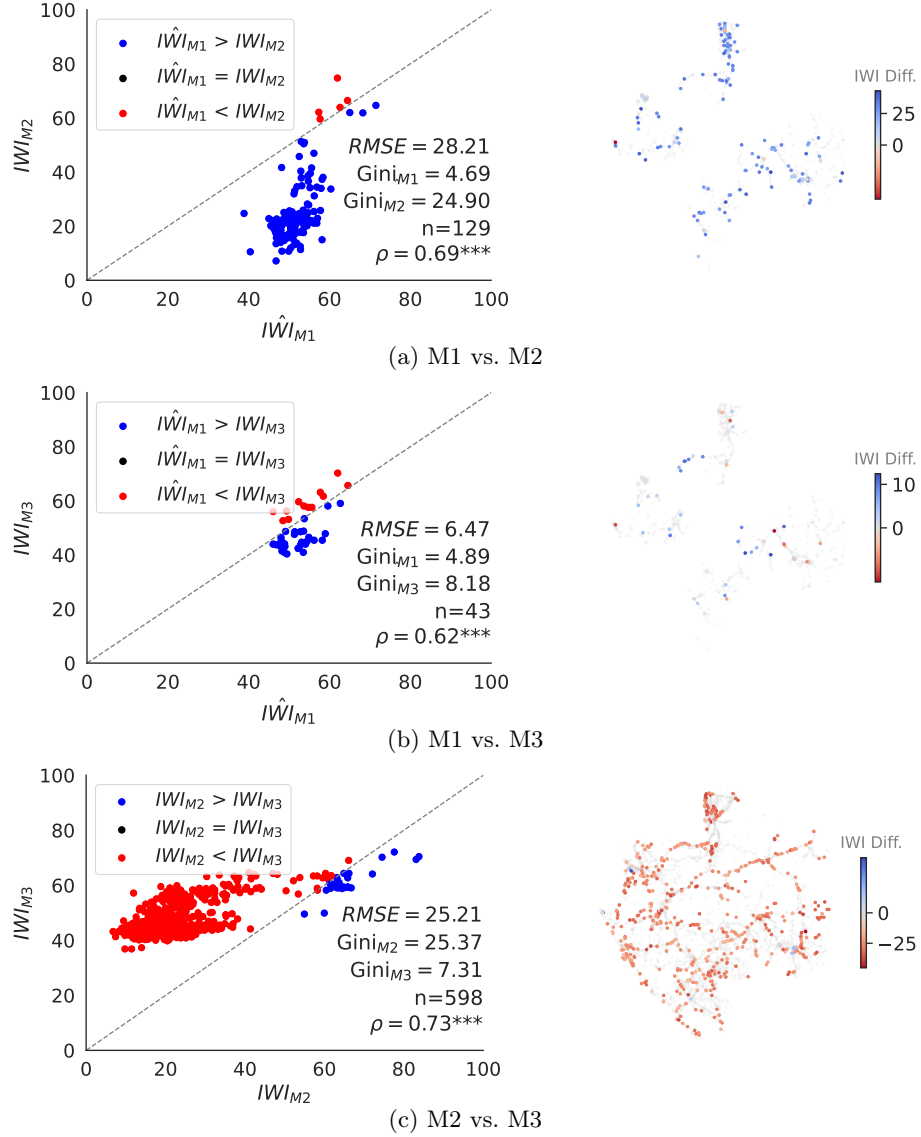


Fig. A10: IWI predictions in overlapping locations in Gabon, GAB (M3: $CNN_a + CB$). Right: IWI differences between the predictions of two models for each overlapping location. Left: Correlation between these predictions. Colors indicate the direction of the differences. M2 generally underestimates wealth compared to M1 (blue in (a)) and M3 (red in (c)). Predictions from M1 are more homogeneous than M2 and M3. In (c), M2's predictions are more heterogeneous than M3's.